



ELSEVIER

Available online at www.sciencedirect.com

SCIENCE @ DIRECT®

Journal of Sound and Vibration 275 (2004) 151–175

JOURNAL OF
SOUND AND
VIBRATION

www.elsevier.com/locate/jsvi

Effect of unequal Y-pipes on sound propagation in the exhaust system of V-engines

A. Selamet^{a,*}, V. Kothamasu^a, Y. Jones^a, T.C. Lim^b

^a *Department of Mechanical Engineering and Center for Automotive Research, Ohio State University,
206 West 18th Avenue, Columbus, OH 43210-1107, USA*

^b *Department of Mechanical, Industrial and Nuclear Engineering, University of Cincinnati, 624 Rhodes Hall,
P.O. Box 210072, Cincinnati, OH 45221-0072, USA*

Received 1 July 2002; accepted 23 June 2003

Abstract

The crossover or the Y-pipe that connects the two banks of a V-engine to a single exhaust duct in vehicles play a significant role in the relative arrival times of the primary pressure pulses in the Y-connector, thereby affecting the tailpipe-outlet sound quality. To quantify this behavior at full as well as part-load, dynamometer experiments are conducted on an even firing General Motors 4.3L V6 engine with two different crossover pipes: one with unequal and the other with equal branch lengths. The instantaneous crank-angle resolved pressure data is acquired simultaneously both inside the exhaust duct and externally at the tailpipe outlet. The in-duct measurements employ a piezoresistive pressure transducer, while the external tailpipe-outlet measurements use a binaural acoustic head. The significant impact of the branch-length inequality is established by examining the in-duct order content and tailpipe-outlet sound quality. © 2003 Elsevier Ltd. All rights reserved.

1. Introduction

Extensive use of V-engines in contemporary vehicles brings about the importance of the approach in combining the two separate banks through a crossover pipe, or often referred to as a Y-pipe. It is a well-known fact for symmetric (or, equivalently, even) firing engines that the unequal lengths of two branches of the Y-pipe result in undesirable odd orders of noise due to different travel times of the exhaust blowdown pulses arriving at the Y-connector with unequal intervals. This is true for majority of the V-engine designs with symmetric firing where blowdown pulses continuously switch from one bank to the other for subsequent power strokes. A similar

*Corresponding author. Fax: +1-614-292-3163.

E-mail address: selamet.1@osu.edu (A. Selamet).

uneven pulse distribution in the Y-connector may also be produced by odd firing engines despite the equal length Y-branches [1]. Since the majority of the designs, however, involve the former category of equal firing and unequal length branch pipes, the present study concentrates on this category of engines and Y-pipes.

Numerous aspects of noise propagation and cancellation in engine exhaust systems have been studied in detail [2–8], yet the acoustics and noise quality perception due to the varying lengths (unequal vs. equal) of Y-pipe branches have received little attention in the literature. The objective of the present experimental study is then to investigate the effect of this length inequality in the crossover pipe on the acoustic characteristics of the exhaust in-duct pressure and the external tailpipe noise. A General Motors 4.3L V6 Vortec engine is used in the experiments with two different exhaust configurations: (1) a baseline exhaust system with Y-pipe branches of unequal length, and (2) a modified Y-pipe with equalized branch lengths. An experimental setup is developed in an engine dynamometer laboratory to perform simultaneous measurements of internal and external sound pressures (Fig. 1). The in-duct pressures from equal and unequal branch systems are compared in terms of the temporal and spectral information, clearly demonstrating the difference in acoustic behavior between the two systems. The tailpipe noise attributes of major significance are quantified by employing a number of signal processing schemes [9], including analysis of spectrogram response and discrete order tracking as well as the application of several metrics. The results (1) confirm the observations on in-duct measurements in terms of the impact of Y-pipe branch lengths on integer and half engine-firing orders, and (2)

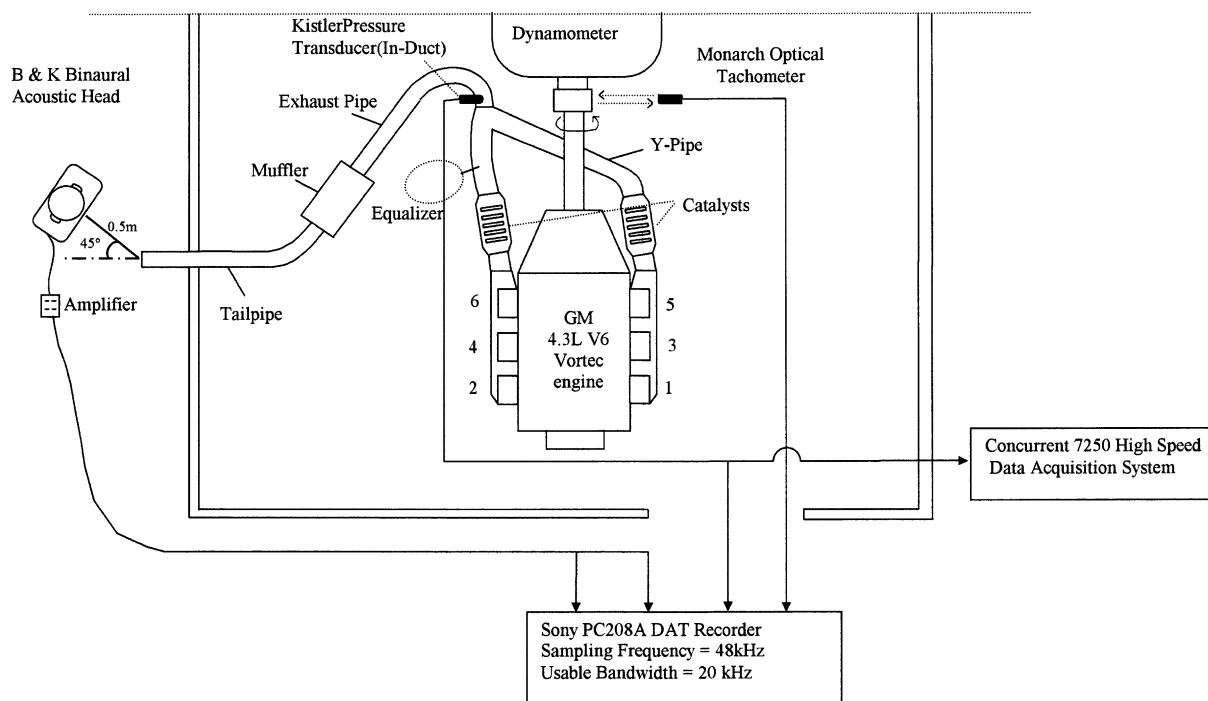


Fig. 1. Schematic of the exhaust noise measurement setup.

reveal how these orders affect noise quality perception. The analysis also leads to the identification of a band-limited roughness-based metric that correlates relatively well to subjective perception.

Section 2 briefly describes the engine dynamometer setup and Section 3 discusses the time-averaged engine performance parameters. Section 4 presents the findings based on the in-duct time-resolved pressure measurements and Section 5 the external tailpipe measurements and the sound quality analysis as applied to these results. After a short discussion of flow noise in Section 6, the study is concluded in Section 7 with final remarks.

2. Engine dynamometer setup

A General Motors Vortec 4300 V6 engine (bore = 101.60 mm, stroke = 88.39 mm, and compression ratio = 9.21) is used in an engine dynamometer facility with full vehicle exhaust system, including one catalytic converter on each bank of the Y-pipe and a muffler. Experiments are conducted with two different Y-pipe configurations to determine the impact of inequality of the crossover pipe length on sound quality. A schematic of the exhaust system, including the Y-pipe with catalysts and the exhaust pipe with muffler, is shown in Fig. 1, while deferring the detailed dimensions to Fig. 22 of Appendix A. The Y-pipe junction segment has been modified in this study to accommodate an equalizer on the short branch (right bank). The junction of the Y-pipe is rotated 90° relative to the baseline orientation with the equalizer. Thus, the design allows interchangeability between the original unequal-length baseline Y-pipe and the (modified) equal-length baseline + equalizer Y-pipe. The length inequality in branch pipes of the baseline setup was 21.25 in. With the equalizer installed, the right bank pipe length comes to within less than 1 in (0.75 in longer) of the left bank. The original exhaust pipe lengths as well as a baseline intake system have been retained the same in both experiments. The tailpipe reaches the ambient through the test cell wall and the tailpipe length has also been retained the same.

The data are collected for engine speeds varying from 1000 to 4500 r.p.m. in increments of 500 r.p.m. While the wide-open-throttle (WOT) experiments are emphasized, a corresponding set of data are also acquired for 35% open throttle operation (part-load) primarily for external sound analysis. Exhaust in-duct pressure is measured at the end of the Y-pipe (at the beginning of single exhaust pipe) with a water-cooled piezoresistive Kistler 4045A2 pressure transducer. This in-duct measurement location at the beginning of the single exhaust pipe will hereafter be referred to as the “connector” location. The details of the engine and dynamometer controls along with the data acquisition system of the engine laboratory have been described elsewhere [6] and will not be elaborated here. For sound quality analysis, the tailpipe noise and crank-shaft rotational speed recorded by a B&K binaural acoustic head measurement instrument and a Monarch optical tachometer, respectively, to determine the effect of equal vs. unequal exhaust runner lengths on sound quality perception. The binaural head was located at a distance of 0.5 m from the tailpipe outlet with a viewing angle of 45° as shown in Fig. 1 along with the approximate position of the optical tachometer that was used to sense one pulse per revolution of the output shaft. The measurements of tailpipe noise (2 channels), engine speed, and in-duct pressure signatures have been synchronized in time by recording all 4 channels simultaneously into a high spectral-bandwidth Sony PC208 DAT recorder. The data was sampled at 48 kHz that resulted in an audible bandwidth of at least 20 kHz. Even though the spectral range of primary interest is mostly

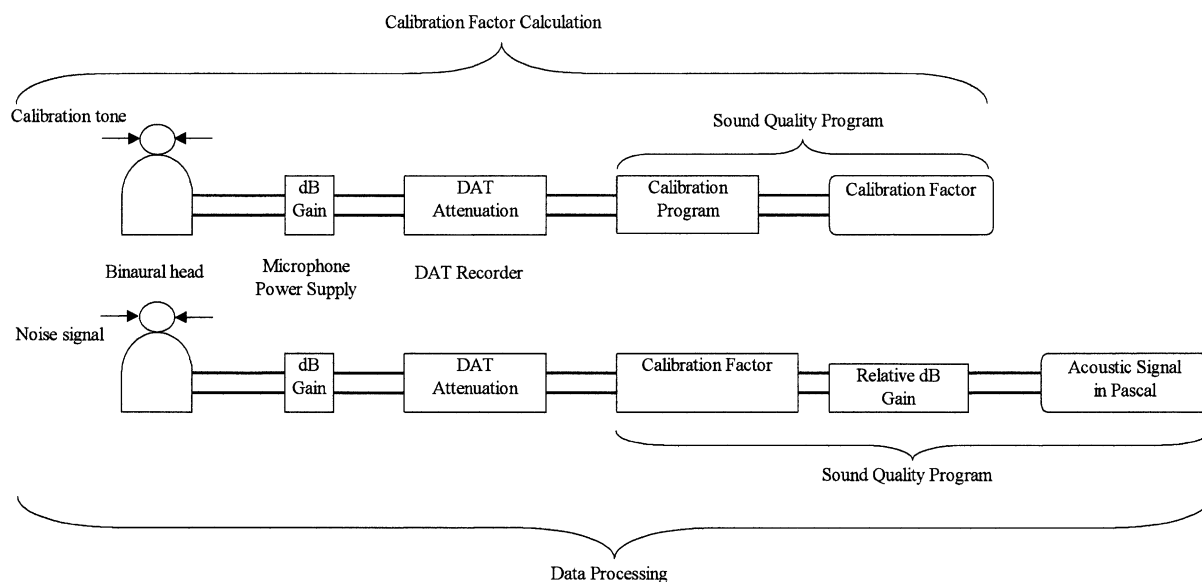


Fig. 2. Digital signal calibration and processing scheme for binaural acoustic head measurement of tailpipe noise.

below 1 kHz, the higher frequency contents are acquired and stored in the time-domain ranging from 30 s to a couple of minutes for realistic subjective perception studies. Prior to the first measurement and also upon completion of the last run, a set of calibration tones for the binaural acoustic head channels are recorded to determine the absolute sound pressure levels during the tests. This is accomplished by computing the exact calibration factors or sensitivity levels of this measurement setup from the calibration tones. The raw data from the DAT tape is then digitized with no loss of frequency resolution, and downloaded into an advanced signal processing system for data storage and further processing in time, frequency, and engine-related order domains. This procedure is summarized in Fig. 2.

3. Engine performance

The brake torque and power generated by the engine at WOT are depicted in Figs. 3 and 4, respectively. The difference between the baseline system (solid line) and the baseline plus equalizer system (dashed line) may be viewed as within the repeatability bounds of the experiments. Thus, the effect of equalizer on the engine performance appears to be negligible.

Figs. 5 and 6 compare WOT and 35% open-throttle values for total mass (air plus fuel) flow rate through the engine and the torque, respectively. Each figure also presents the data for baseline (solid line), as well as baseline plus equalizer (dashed line) systems. Note particularly the difference in mass flow rate in Fig. 5 as the engine speed increases. The restriction in the mass flow rate with increasing engine speed is clearly reflected in the torque curve of Fig. 6. The decrease in mass flow rate may then be related to a decrease in velocity. The implications of this reduction will be discussed later in Section 6 in connection with the flow noise characteristics.

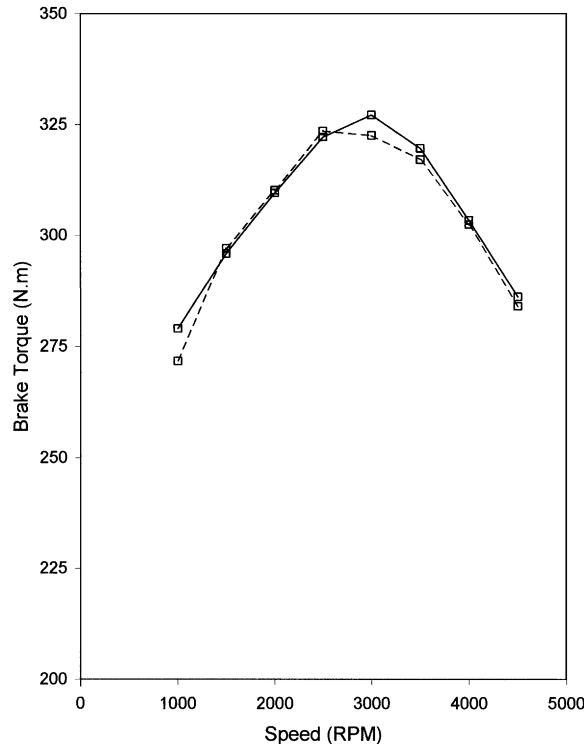


Fig. 3. Effect of equalizer on the brake torque at WOT: $-\square-$, baseline; $--\square--$, baseline + equalizer.

4. Duct measurements and analysis

4.1. Instantaneous pressure and spectral analysis

Figs. 7–9 represent the characteristics of exhaust gas pressure at the connector location (recall Fig. 1) for WOT operation in pairs at relatively low (1500 r.p.m.), mid (3000 r.p.m.), and high engine speeds (4500 r.p.m.), respectively. In view of the firing order of the engine (1–6–5–4–3–2) and the reference chosen for the crank angle axis, the cylinder numbers associated with each major pulse have been superimposed on these figures. First figure in each pair (Fig. 7(a), for example) depicts the absolute pressure vs. time (crank angle) and the second figure (Fig. 7(b), for example) shows the corresponding Fourier transformation in the sound pressure level (SPL)-order domain. The first order is defined as $n/60$, where n is the crank-shaft speed in r.p.m. Any other order is a multiple of the first order. Each figure also combines the baseline system with unequal Y-pipe (solid line) and the modified baseline system with equalizer (dashed line). The pressure–time traces of Fig. 7(a) show that the equalizer (1) eliminates the secondary peaks, and (2) delays the arrival of blowdown pulses from cylinders 2, 6, and 4 on the right bank (short bank in the production system), thereby facilitating a more even distribution of pulses in the crank-angle domain. The amplitudes of all primary peaks are only slightly modified. When this information is transformed into the frequency domain of Fig. 7(b), the half-orders, including the 1.5, 4.5, and 7.5, of the

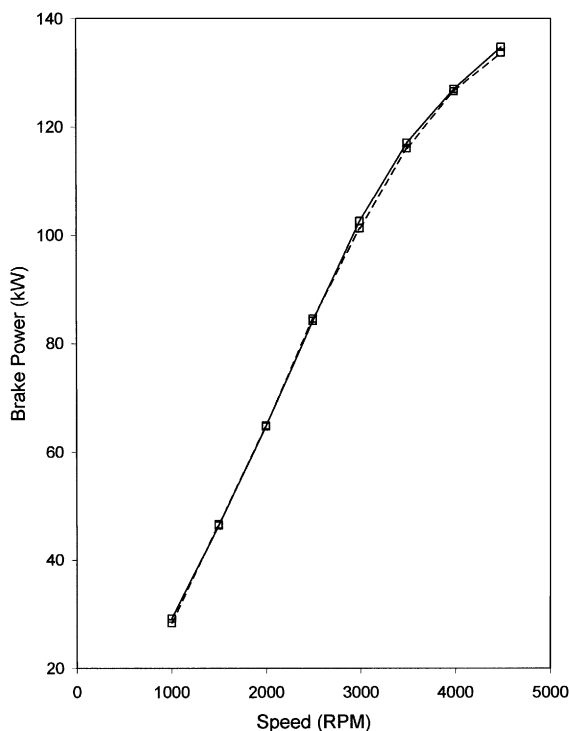


Fig. 4. Effect of equalizer on the brake power at WOT: $-\square-$, baseline; $--\square--$, baseline + equalizer.

unequal baseline system have been significantly reduced by the equalizer, while retaining the same magnitude for the fundamental (third order). Similar trends in terms of pulse arrival delays and comparable amplitudes are observed with increasing engine speed in Figs. 8(b) and 9(b). The behavior at high engine speed 4500 r.p.m. becomes more distinct in that the pressure–time curve exhibits predominantly 3 peaks for the baseline exhaust system, leading to a rather strong 1.5 order followed by 4.5 and 7.5 orders in Fig. 9(b). Note in Fig. 9(a) that the introduction of an equalizer brings 6 pulses back, which reduces the magnitude of all half orders as observed in Fig. 9(b).

The foregoing experiments were repeated for a part-load operating condition with a 35% throttle body opening. The results at this setting corresponding to Figs. 7–9 are depicted in the same order in Figs. 10–12. In general the trends at part-load, particularly at low engine speeds, is similar to the WOT operation. The effect of the equalizer in terms of reducing the half-orders remains the same with part-load operation. The differences between the two operating conditions become observable, however, with increasing engine speed. For example, comparison of Figs. 12 and 9 reveals an important difference in the amplitude of pressure oscillations. Decreasing amplitudes with throttled operation and increasing engine speed are expected, due to the lower mass flow through the engine. The motivation for part-load experiments as well as the implications will become more clear later in Section 5 in the analysis of the tailpipe-outlet sound signature.

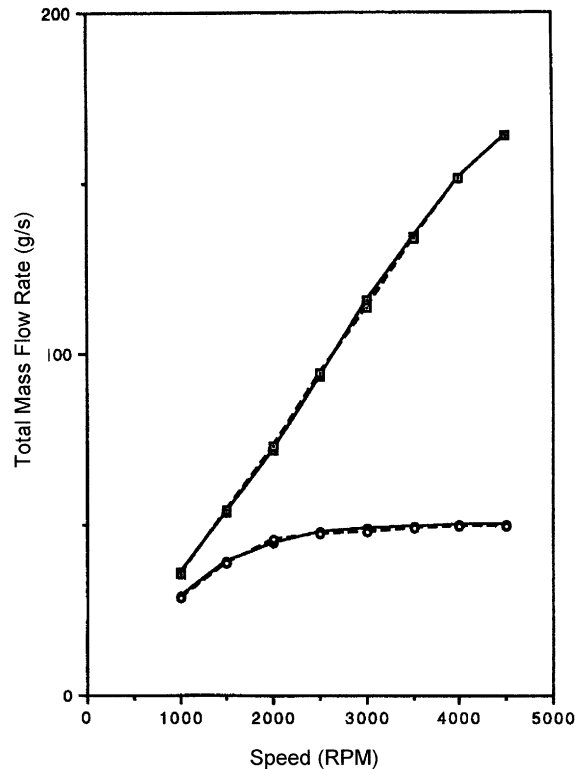


Fig. 5. Total mass (air + fuel) flow rate in the baseline exhaust and baseline + equalizer exhaust systems at WOT and 35% throttle open: —□—, 100% throttle (baseline); —○—, 35% throttle (baseline); --□--, 100% throttle (baseline + equalizer); --○--, 35% throttle (baseline + equalizer).

4.2. Order tracking

A useful alternative to the frequency-domain information presented in the preceding section is to track specific orders as function of engine speed. Fig. 13 compares the SPL of the baseline system and the baseline system with the equalizer for integer orders, including 3, 6, and 9. For most of the speed range, the equalizer tends to strengthen the integer orders. This trend is weak for the important fundamental (third) order in terms of magnitude, whereas it becomes more pronounced with less important increasing orders. Fig. 14 presents a consistent reduction in all of the half-order amplitudes due to the presence of the equalizer at all engine speeds. The reduction appears to be most pronounced for the 1.5 order particularly at higher engine speeds, and continues to persist with increasing orders, although somewhat weakened at the 7.5 order. A careful inspection of the relative contributions of different orders to the overall SPL reveals that (1) the fundamental (third) order is clearly the dominant one; (2) the SPL of a specific integer order decreases with increasing order throughout the speed range; (3) the results of half-orders are not that unified particularly at low engine speeds: above 2000 r.p.m., the trends in half-orders of the baseline exhaust system are similar to those of integer orders; and (4) with the introduction of

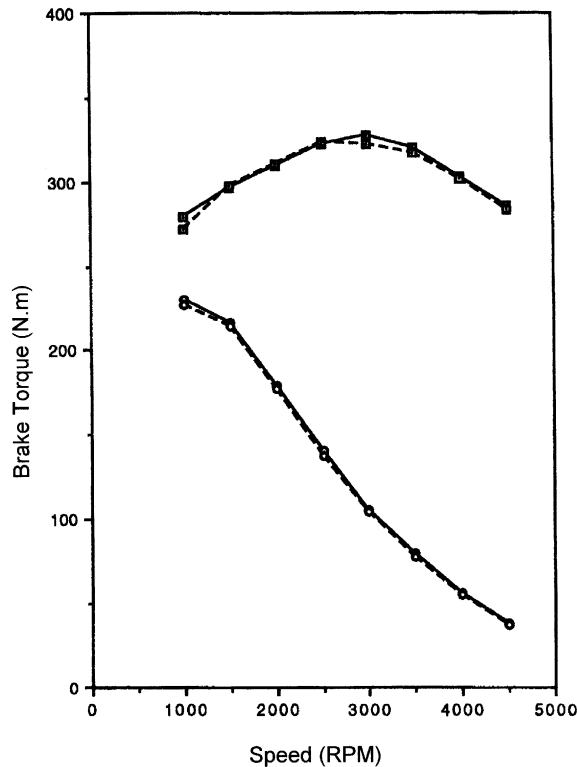


Fig. 6. Brake torque in the baseline exhaust and baseline + equalizer exhaust system at WOT and 35% throttle open: $-\square-$, 100% throttle (baseline); $-\circ-$, 35% throttle (baseline); $--\square--$, 100% throttle (baseline + equalizer); $--\circ--$, 35% throttle (baseline + equalizer).

the equalizer, the magnitudes of half-orders are reduced significantly, which brings all three half-orders somewhat closer (near 140 dB).

The foregoing analysis was repeated for the part-load condition of 35% throttle body opening. The details of the results at this operating condition have been excluded for brevity. The basic behavior discussed for the WOT case still holds with some exceptions: For example, (1) higher integer orders in the two exhaust systems have now come closer at part-load, and (2) there is no clear directional trend in terms of relative significance of half-orders with the equalizer.

5. Tailpipe sound quality analysis

5.1. Spectrogram response

Using a short-time FFT-based algorithm for fixed time-window size (based on a block size of precisely 16384 samples with 50% overlap), the near-instantaneous spectrogram response functions of the baseline (with unequal pipe length) and modified (with equalizer) exhaust systems

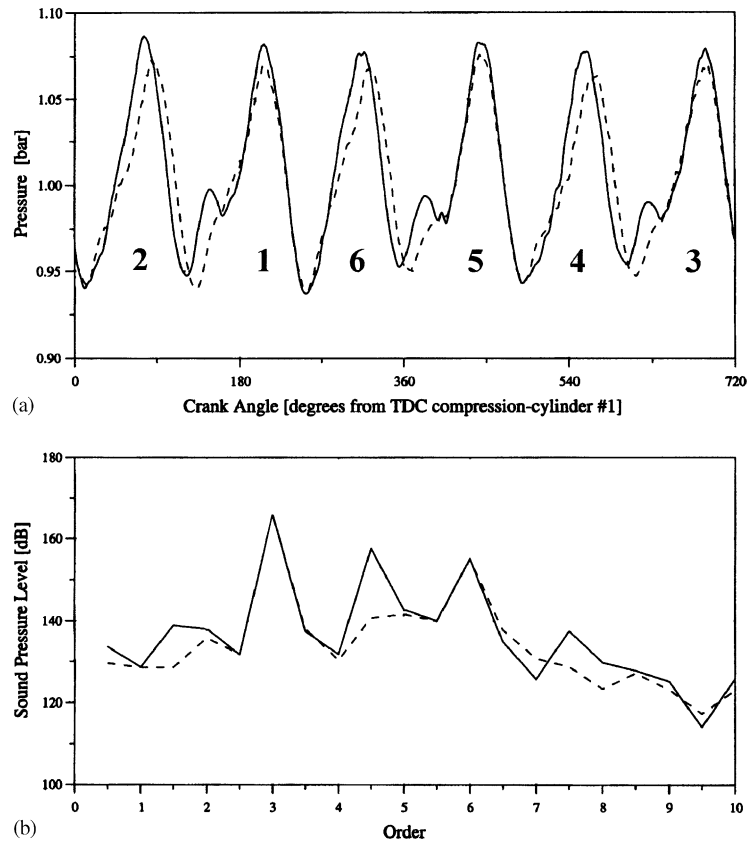


Fig. 7. Effect of equalizer at the connector location at 1500 r.p.m. and WOT: (a) pressure vs. crank angle and (b) SPL vs. order. —, Baseline exhaust; ---, baseline + equalizer.

are computed. The spectrogram results are illustrated in terms of engine order versus time in Figs. 15(a)–(d) and (e)–(h) for full (100% open throttle) and part (35% open throttle) load, respectively. Each spectrogram has a number of relatively straight horizontal lines of intense sound pressure levels above the broadband background noise. These order lines represent the instantaneous peak response spectrum of the measured tailpipe noise. The color intensity specified by the horizontal bar chart of the spectrogram plots gives the amplitudes of the measured sound pressure data from the binaural acoustic head microphones. Only the right-ear microphone data are used here since the analysis essentially shows similar trends from both artificial ears. Qualitatively, the response functions from the baseline exhaust system exhibit the strong presence of half- and integer orders. On the other hand, the equalized system nearly eliminated all half-orders, while retaining the approximate level of intensity of the integer orders. To better quantify the amplitudes of each discrete order peaks corresponding to the primary crank-shaft rotation frequency and its first 10 harmonics, a flattop window has been applied. Fig. 15 also specifically shows comparisons of right-ear spectrogram response functions of the baseline and equalized systems for two selected steady state engine speeds (1500 and 3000 r.p.m.) for full and part load.

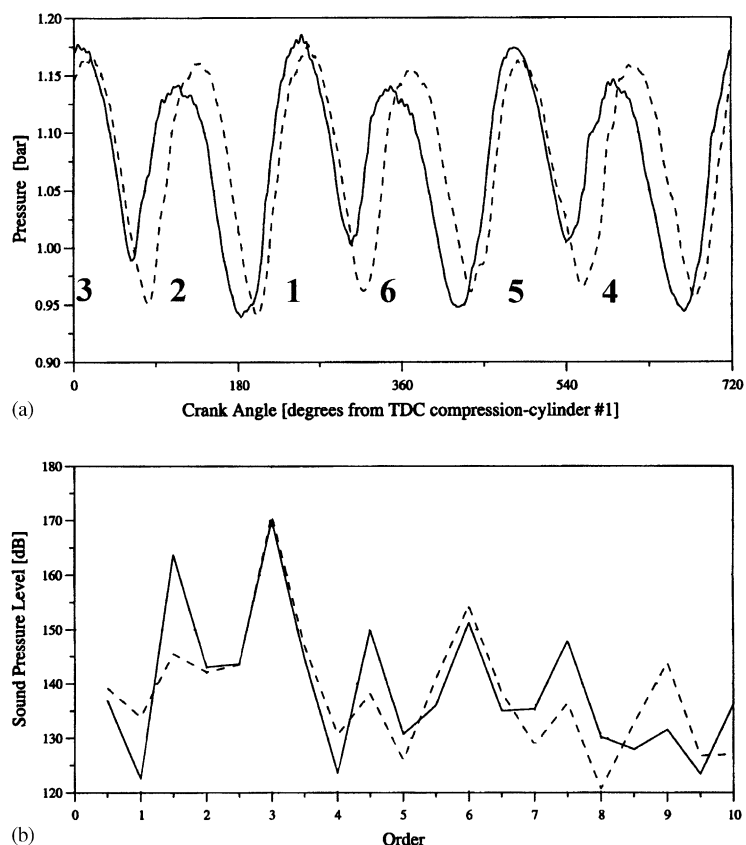


Fig. 8. Effect of equalizer at the connector location at 3000 r.p.m. and WOT: (a) pressure vs. crank angle and (b) SPL vs. order. —, Baseline exhaust; ---, baseline + equalizer.

The baseline exhaust system with unequal branch lengths in Figs. 15(a),(c),(e) and (g) shows collectively 6 distinct lines corresponding to 1.5, 3, 4.5, 6, 7.5, and 9 orders. The modified system with equal branch lengths in Figs. 15(b),(d),(f) and (h) however, produces only 3 visible distinct lines corresponding to 3, 6, and (at times) 9 orders. The half-orders in the latter are rather weak and hardly noticeable. Qualitatively, the integer orders of the equalized system are typically a little more intense than those of the baseline system. This characteristic is generally consistent throughout the entire speed range similar to the in-duct pressure results. Since half-order contents are known to produce a low-frequency rumble sensation which deteriorates the sound quality of the exhaust noise, and also integer orders are often more acceptable subjectively [10], the modified equalized system may be considered a “better design” than the baseline system. This effect is quantified by a proposed set of metrics introduced later in Section 5.3. In addition, the broadband background noise increases with engine speed and is found to be practically the same for both exhaust configurations. Even though this background noise is more intense in the right-ear microphone data, the order-related peak responses of both ears are nearly the same in amplitude. Later, this background noise will be discussed further in relation to the perceived sound quality.

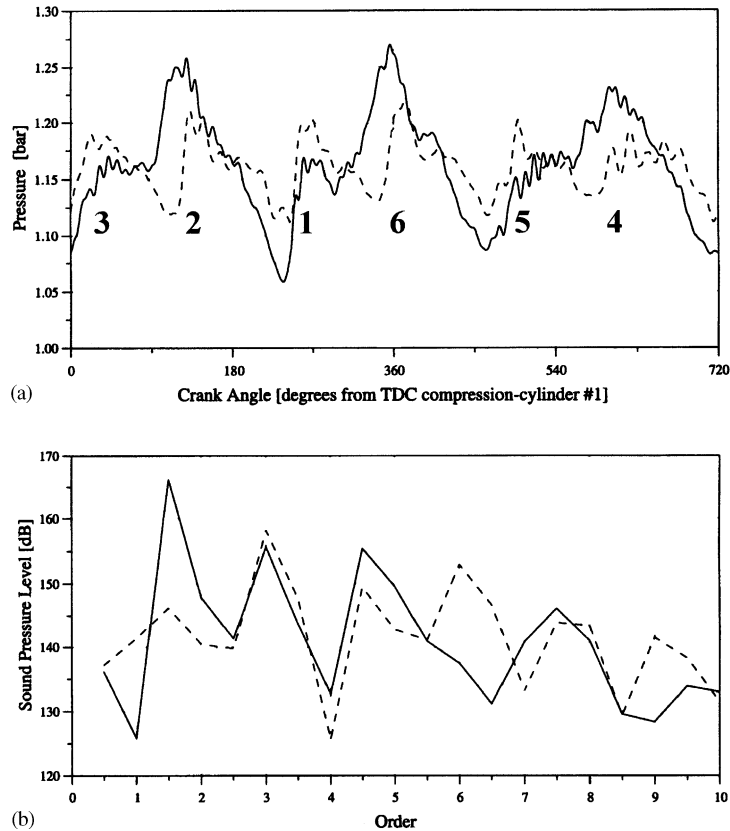


Fig. 9. Effect of equalizer at the connector location at 4500 r.p.m. and WOT: (a) pressure vs. crank angle and (b) SPL vs. order. —, Baseline exhaust; ---, baseline + equalizer.

5.2. Discrete order tracking

The spectrogram functions readily reveal the overall quality and characteristics of the exhaust noise signatures, since they provide a complete instantaneous representation of the data in both time and frequency domains. However, to obtain a more precise time-averaged quantitative response of the sound pressure data, the method of synchronized discrete order tracking is applied. The temporal signatures are first sub-divided into blocks that make up one engine cycle (2 crank-shaft revolutions.) Then a time-domain averaging is performed that is synchronized with the angular displacement of the crank-shaft. The resulting time record is based on the sample length of one cycle at a particular speed. Thus, its actual temporal range is a function of the steady state engine speed. For example, a time range of 0.12 s corresponds to an engine speed of 1000 r.p.m. The reduced temporal data points are then used to compute a clean order domain response by applying the conventional FFT algorithm. These calculations are performed on the complete set of raw noise signals acquired from the baseline and modified exhaust experiments. The results for the same two engine speeds at full load are shown in

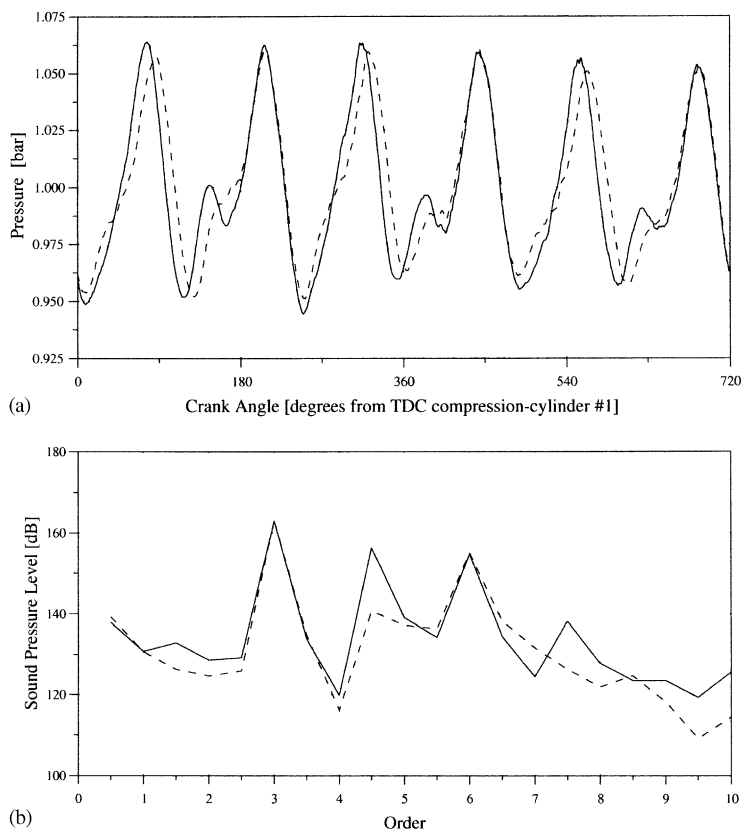


Fig. 10. Effect of equalizer at the connector location at 1500 r.p.m. and 35% throttle open: (a) pressure vs. crank angle and (b) SPL vs. order. —, Baseline exhaust; ---, baseline + equalizer.

Fig. 16 with a pair of graphs shown for each speed and configuration. The temporal plots are the detailed time–history functions of the right-ear sound pressures for one cycle. The spectral graphs correspond to engine-related order response functions. A peak is observed at every half-order, a characteristic of the dynamics of rotational machinery such as IC engines. The half orders are again much lower in the equalized system, as expected, while only some or no increase is observed in the amplitudes of integer orders. As discussed earlier, the time waveforms of the equalized exhaust are more regular. Similar trends are observed under part-load conditions.

The integer order and half-order peak levels at full load for each engine speed and exhaust system are compared in Figs. 17 and 18, respectively. Note that the relative dependency on speed does not change significantly when the unequal branch lengths are equalized. Yet, a drastic reduction is observed in the amplitudes ranging from approximately 5–15 dB. The amplitude reduction in the 1.5 and 4.5 orders is observed to be more significant than the decrease seen in the 7.5 order. Overall, the relative trends in these external sound signatures resemble those in Figs. 13 and 14 for the in-duct pressures.

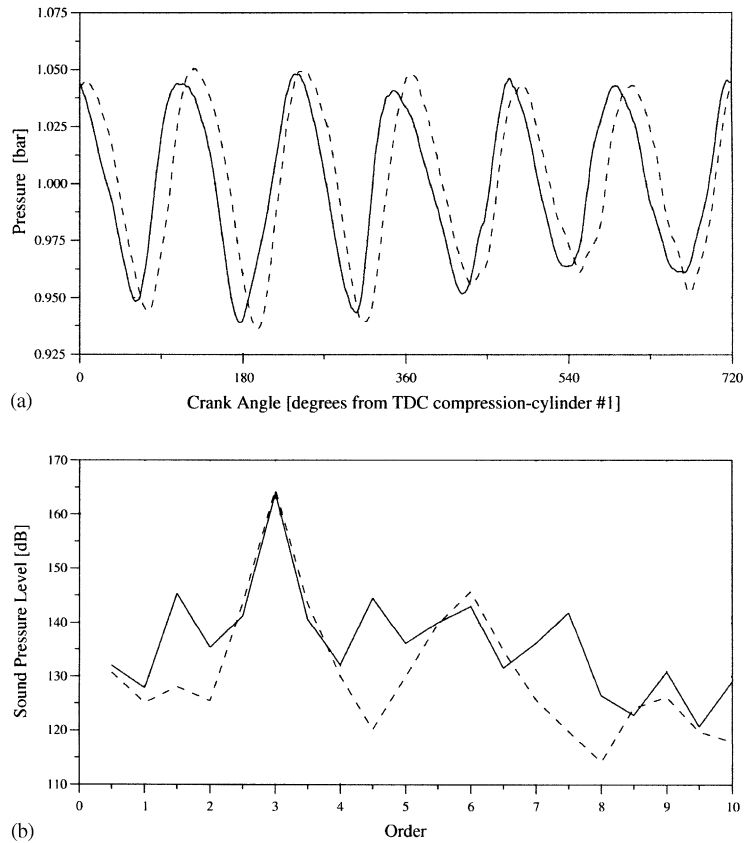


Fig. 11. Effect of equalizer at the connector location at 3000 r.p.m. and 35% throttle open: (a) pressure vs. crank angle and (b) SPL vs. order. —, Baseline exhaust; ---, baseline + equalizer.

5.3. Sound quality metrics

With the digitized temporal waveforms that preserve the full audible bandwidth, a wide range of subjective playback, real-time signal processing and visualization analysis can be performed, including back-to-back comparative-listening sessions, semantic differential experiments, and digital filtering studies. In the present study, primarily dual and multiple comparative-listening programs are used to conduct subjective analysis of the tailpipe noise from the baseline and equalized exhaust systems with the engine running at numerous steady state speeds. These analyses coupled with simultaneous critical visualization of the time–frequency response functions helped understand the effect of half and integer orders on sound quality and its perception. These subjective studies revealed that the tailpipe noise quality at the lower and mid engine speed range is affected most significantly by half-orders. At higher speeds and full load, the half-order response is not the only dominant negative attribute. Here, it is believed that flow noise contribution becomes quite significant as well. The contributions from each component (half-orders, integer orders and broadband noise) are determined by using a variety of digital filters

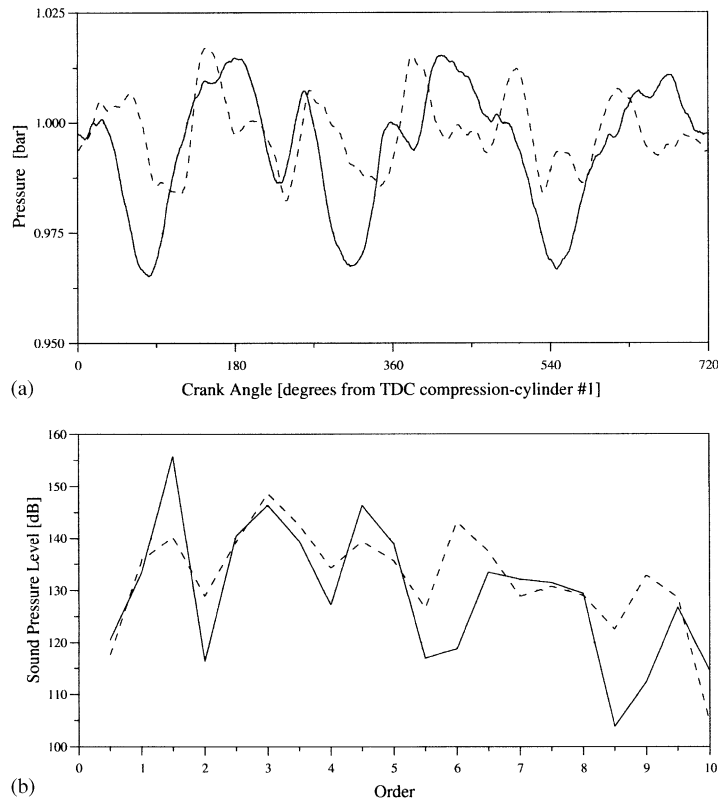


Fig. 12. Effect of equalizer at the connector location at 4500 r.p.m. and 35% throttle open: (a) pressure vs. crank angle and (b) SPL vs. order. —, Baseline exhaust; ---, baseline + equalizer.

such as low pass and band pass. These filters are applied in real-time playback mode to either enhance or suppress specific attributes to isolate their effects and better understand their perceived influences.

Although it is useful to perform subjective listening and visualization studies, the ability to quantify specific noise characters is also highly desirable by using suitable metrics. Four types of sound quality metrics are applied here to the measured data: Zwicker loudness in sone, speech interference level in dB, relative spectral balance in dB, and roughness in asper. This set of metrics is usually available in sound quality software packages [11]. The first 2 metrics are relatively standard and have been used widely, whereas the last 2 are not as common, and significant differences may be observed in the absolute levels from different software packages. However, due to the quasi-steady state nature of the present data, the relative trends should be very similar regardless of the specific algorithms used. A brief explanation of each metrics is given next.

Loudness is a measure of the perceived intensity of sound. This particular loudness calculation, suggested by Zwicker, is based on the one-third octave band spectra [12]. The second metric on the commonly used speech interference level is a scale to indicate the amount of inhibition to normal intelligible speech in the presence of the noise environment [13]. It is based on the

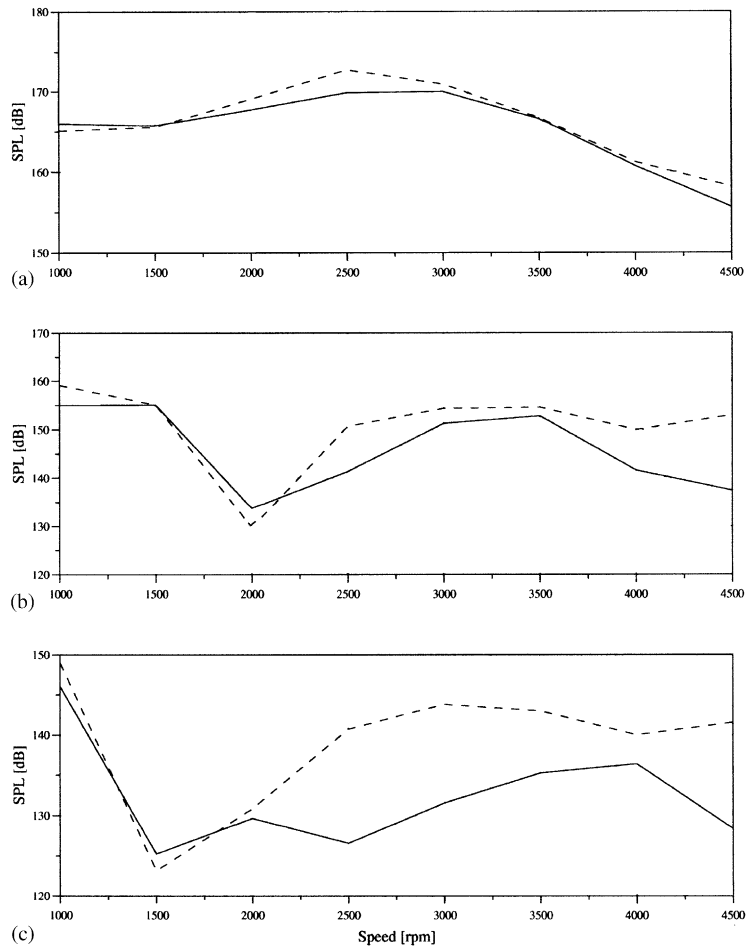


Fig. 13. Effect of equalizer at the connector location on the individual orders as a function of speed at WOT: (a) third order, (b) sixth order and (c) ninth order. —, Baseline exhaust; ---, baseline + equalizer.

arithmetic sum of octave band levels within the speech communication frequency range. Relative spectral balance (RSB) provides a weighted-quantity of the intensity of low-frequency sounds compared to high-frequency contributions. It can be computed as a function of engine speed by $RSB = (\text{Linear SPL}) - (\text{Speech Interference Level})$. The higher values then imply more significant contribution from engine orders, as opposed to higher frequency broadband noise. Lastly, the roughness scale is used to give an indication of the degree of granularity in the sound due to high-frequency modulation (> 20 Hz) of audible noise. The roughness algorithm is fundamentally based on the computational scheme proposed by Aures [14]. The primary difference here is the application of a low-pass filter having cutoff frequency $f_c = 1400$ Hz, and a Q factor of 0.71 (ratio of f_c to Δf at about -3 dB from f_c) and 56 poles (to maximize filter roll-off slope) to the noise data prior to computing the mean roughness level. This calculation actually extracts (band-limited) roughness contribution from noise content within the first 10 engine orders, and simultaneously

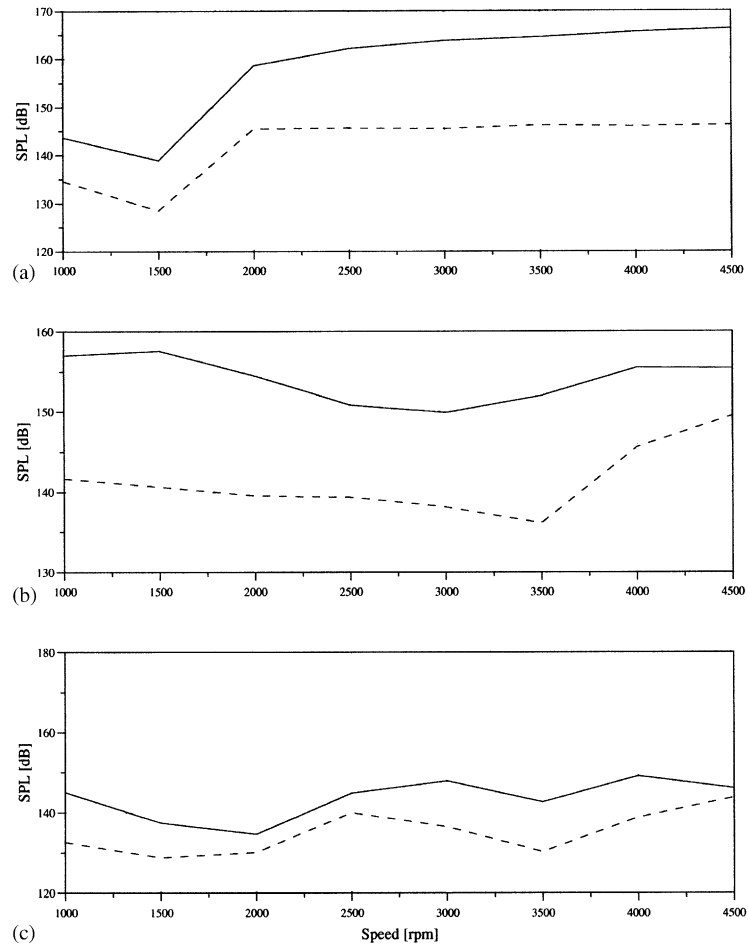


Fig. 14. Effect of equalizer at the connector location on the individual orders as a function of speed at WOT: (a) 1.5 order, (b) 4.5 order and (c) 7.5 order. —, Baseline exhaust; ---, baseline + equalizer.

suppress the contribution from high-frequency broadband noise that can be quite significant especially at higher audible frequencies.

Fig. 19 gives the quantitative values of these 4 metrics for the tailpipe noise at full load in the speed range from 1000 to 4500 r.p.m. Since a metric value can be computed for each ear of the binaural head and the trends are similar, an arithmetic mean is used in the illustrations of the results. The line graphs show that loudness [Fig. 19(a)] and speech interference level [Fig. 19(b)] increases with speed, as expected. Also observed are the slightly higher amplitudes of loudness and speech interference level in the noise response from the baseline exhaust system. However, the variations are not considered significant enough to account for the differences in the subjective perception. On the other hand, substantial differences are found in the computed roughness levels [Fig. 19(d)] when comparing the baseline and equalized systems. Here, the difference between equal and unequal lengths are more significant at the lower engine speeds and less prominent at

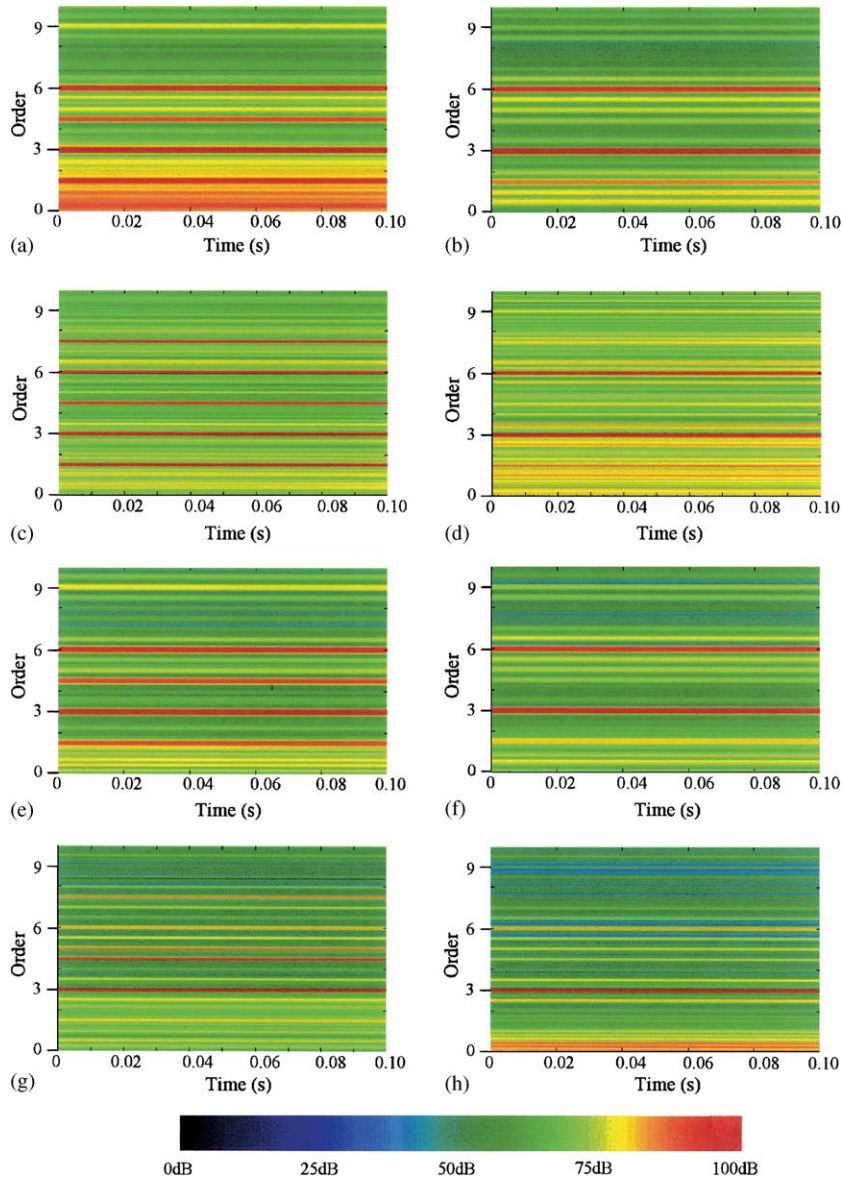


Fig. 15. Comparison of right-ear spectrogram response of tailpipe noise at (a)–(d) full load, and (e)–(h) part load. Baseline exhaust [(a), (e) 1500 r.p.m. (c), (g) 3000 r.p.m.]; baseline + equalizer [(b), (f) 1500 r.p.m., (d), (h) 3000 r.p.m.].

higher speeds, which may be due to the fact that roughness contribution from broadband noise (even though some of the higher frequency components have been suppressed digitally) becomes more dominant at higher speeds. The increase in relative broadband noise contribution unrelated to engine orders is evident from the steady decrease in RSB, which is an indirect measure of the relative effect of engine orders on sound quality as noted earlier, with increasing engine speed.

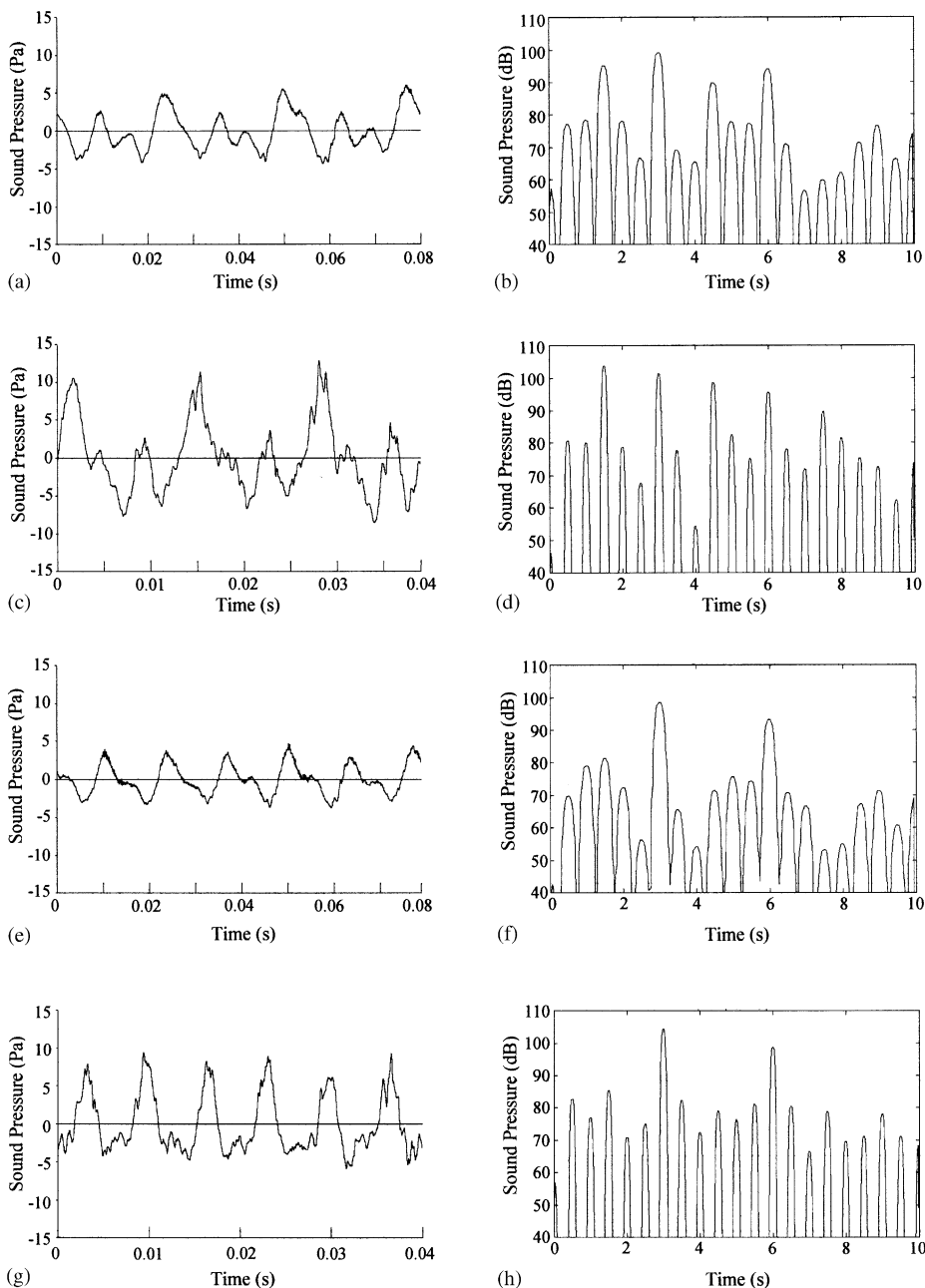


Fig. 16. Temporal and order functions of tailpipe sound pressure levels measured at right-ear under full load condition. Baseline exhaust [(a), (b) 1500 r.p.m. (c), (d) 3000 r.p.m.]; baseline + equalizer [(e), (f) 1500 r.p.m., (g), (h) 3000 r.p.m.].

Qualitatively, the differences in roughness corresponding to the baseline and equalized exhaust systems correlated well to the subjective findings, despite the interference by other non-engine order related sources and characteristics. Thus, the roughness metric applied in this study

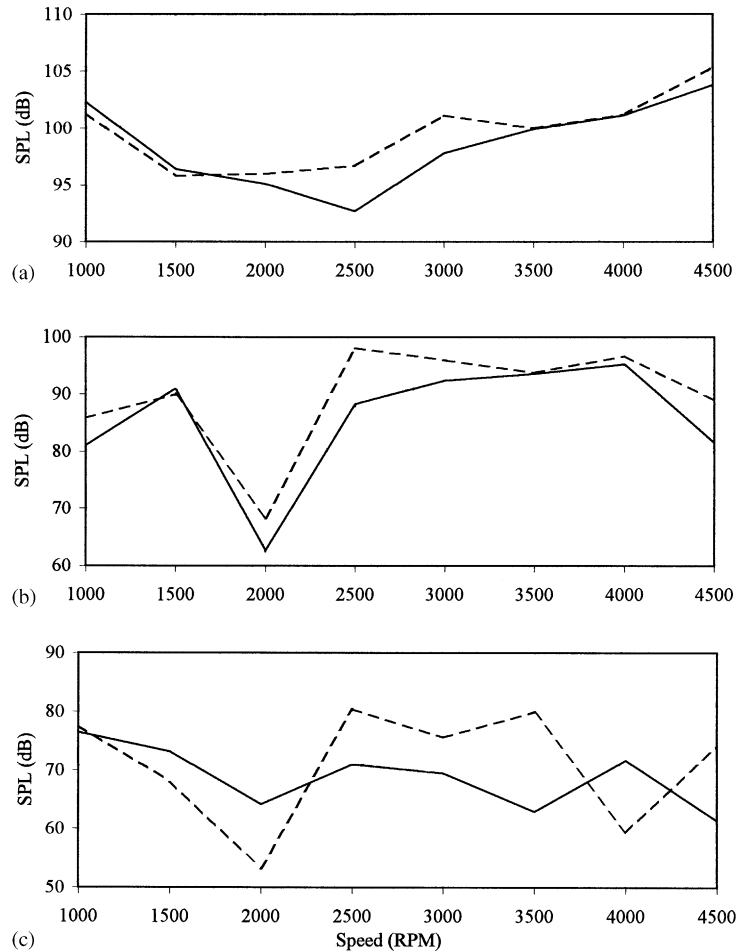


Fig. 17. Discrete order tracking analysis results of integer order structures at full load: (a) third order, (b) sixth order, and (c) ninth order. —, Baseline exhaust; ---, baseline + equalizer.

provides a reasonable measure of the effect of half-orders on rumble sensation, which is generally considered undesirable.

6. Effect of flow noise

While it is not the intention of the present study to evaluate the effects of flow noise, this aspect is still discussed briefly because of its considerable contribution to sound perception, especially at higher speeds and loads. Figs. 20 and 21 show the averaged response of tailpipe noise detected by the binaural head microphones over a wide frequency range (up to 8 kHz) for both full and part loads, respectively. Below 1 kHz, the usual narrowband peaks of the engine firing orders and harmonics are clearly observed. As speed increases, these narrowband peaks move to higher

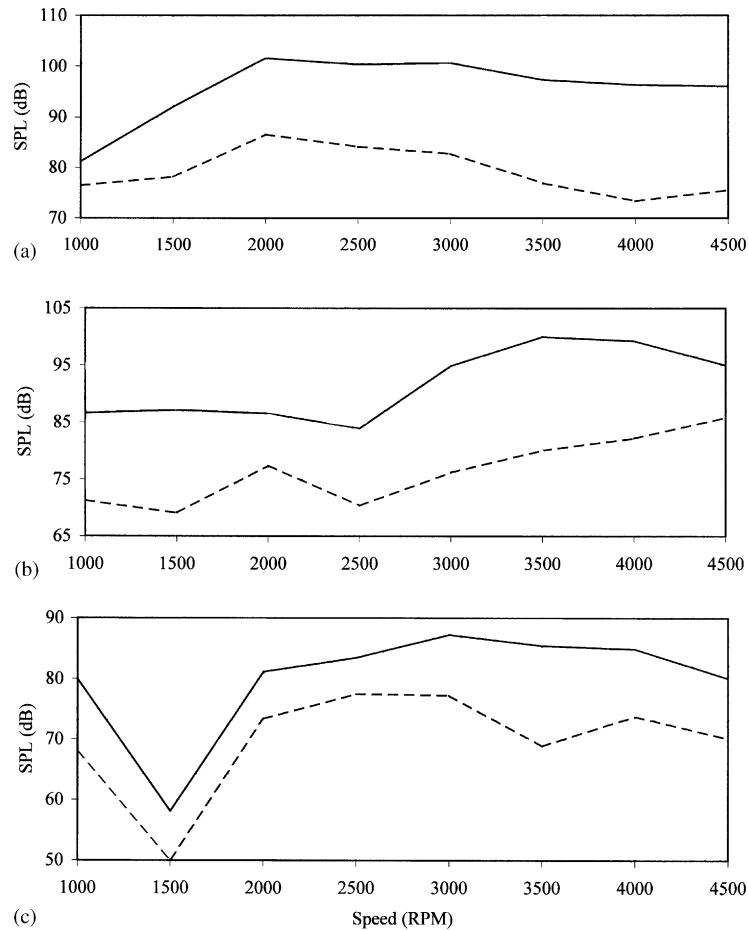


Fig. 18. Discrete order tracking analysis results of half order structures at full load: (a) 1.5 order, (b) 4.5 order, and (c) 7.5 order. —, Baseline exhaust; ---, baseline + equalizer.

frequencies, as expected. Hence, they are clearly functions of the crank-shaft rotational speed. Note that their levels are relatively high reaching more than 100 dB in some cases. There are two other components of this tailpipe noise that are subjectively quite significant: (1) the high-frequency wideband noise observed in the 2–5 kHz range, and (2) the broadband nature and its effect on most of the frequency range shown in these figures, which is observed most clearly above 3000 r.p.m. at WOT, consistent with reference [15]. The overall level is found to increase substantially from 65 to 75 dB between 3000 and 4500 r.p.m. at WOT as shown in Fig. 20. On the other hand, this behavior is no longer observed in the part-load case, where background levels generally stay either the same or even decrease slightly as shown in Fig. 21. The source of these 2 components may be attributed to the noise caused by the fluid flow through internal exhaust elements and tailpipe exit. Further quantification of this behavior requires additional work, and is left to future studies.

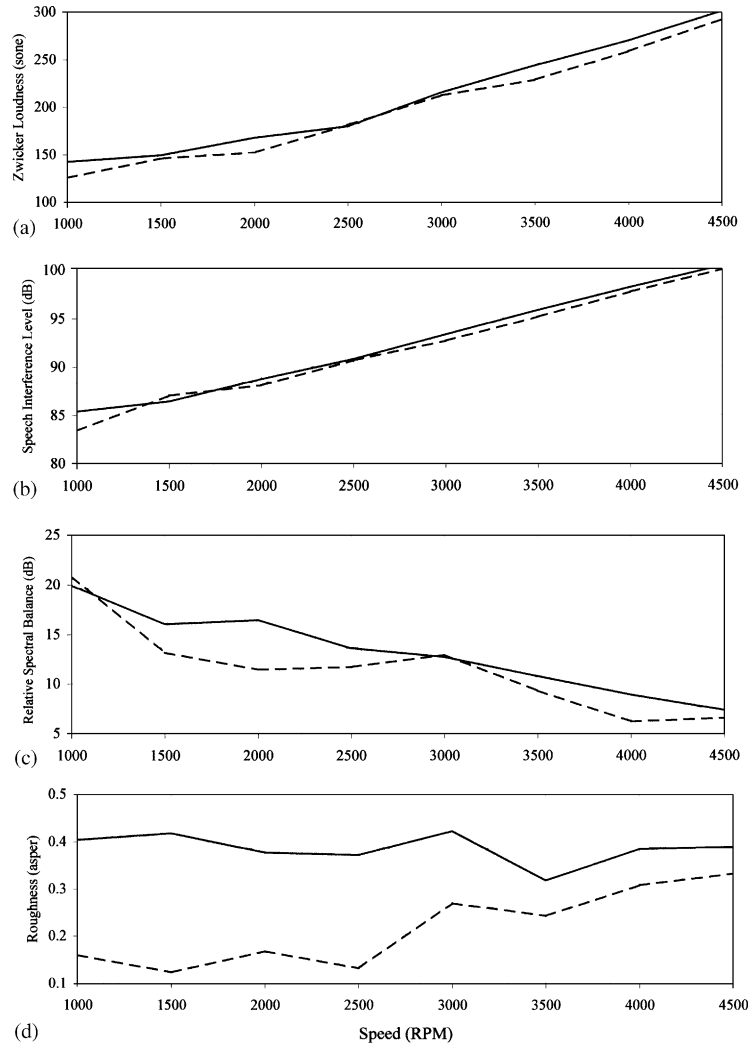


Fig. 19. Predicted sound quality metrics: (a) Zwicker loudness; (b) Speech Interference Level; (c) Relative Spectral Balance; (d) Band-Limited Roughness. —, Baseline exhaust; ---, baseline + equalizer.

7. Concluding remarks

The present experimental study establishes the importance of the relative lengths of Y-pipe branches on the acoustic behavior of the exhaust system in even firing V-engines. A General Motors 4.3L V6 engine is used in the dynamometer experiments with two different crossover pipes: one with unequal and the other with equal branch lengths. The instantaneous crank-angle resolved pressure data is acquired simultaneously by a piezoresistive pressure transducer in the Y-connector and a binaural acoustic head outside the tailpipe. The significant impact of the branch-length inequality is investigated by examining the temporal and spectral behavior

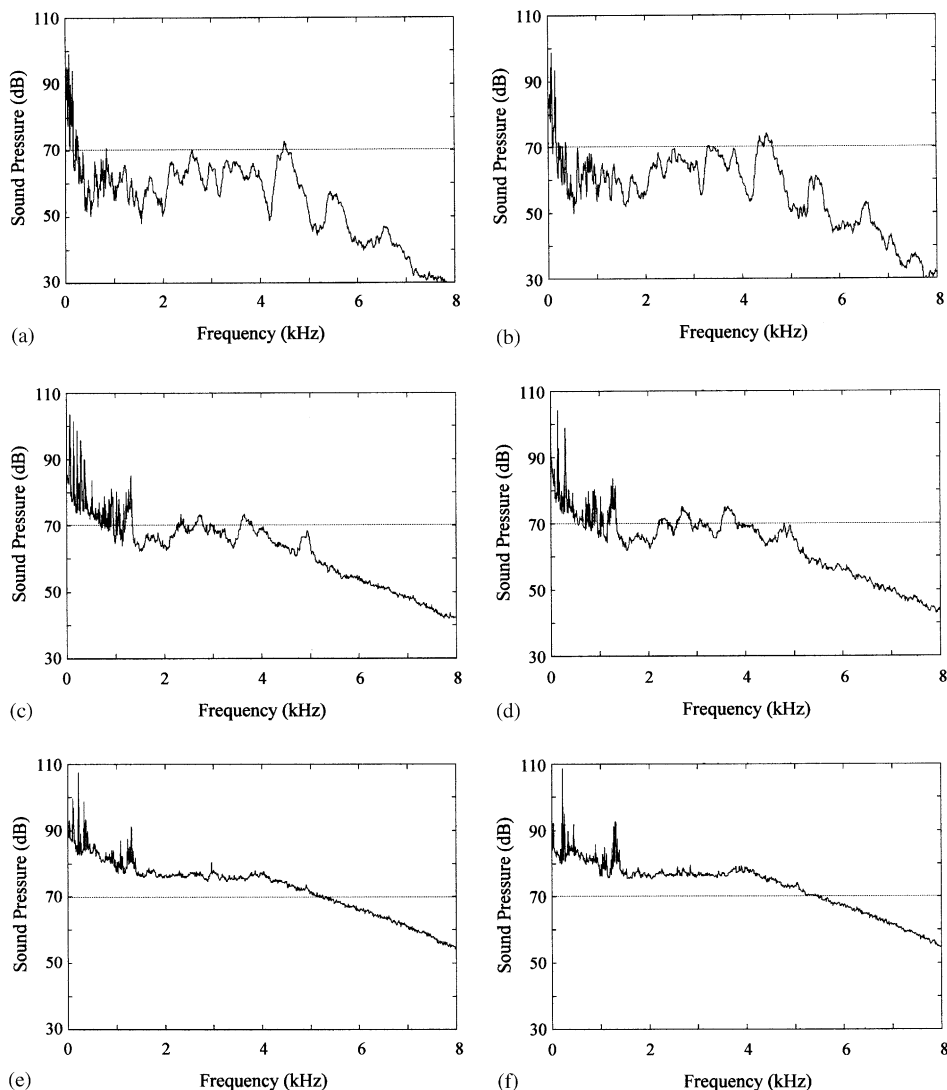


Fig. 20. Effect of low, mid, and high engine speeds at full load on broadband tailpipe noise of the baseline [(a) 1500 r.p.m., (c) 3000 r.p.m., (e) 4500 r.p.m.] and baseline + equalizer [(b) 1500 r.p.m., (d) 3000 r.p.m., (f) 4500 r.p.m.] exhaust systems.

of the in-duct pressure with particular emphasis on the order contents. A series of spectrogram response and discrete order tracking calculations are also applied to the tailpipe noise measurements, as well as a roughness-based noise quality metric. Both analyses clearly show that (1) the half-orders have strong presence in the unequal Y-pipe, which can result in the sensation of roughness annoyance in an exhaust system, and (2) the equalized configuration practically eliminates all of the half-order content. The experimental data also detect the presence of

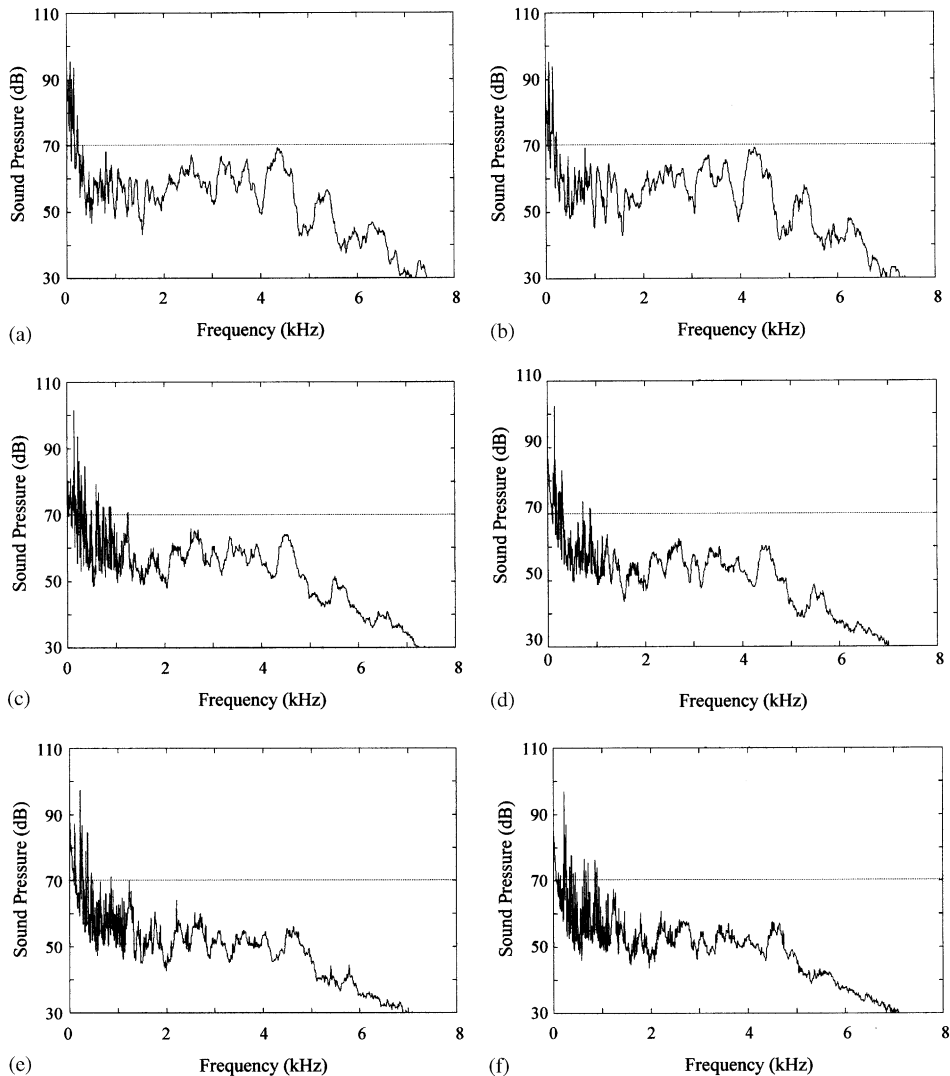


Fig. 21. Effect of low, mid, and high engine speeds at part load on broadband tailpipe noise of the baseline [(a) 1500 r.p.m., (c) 3000 r.p.m., (e) 4500 r.p.m.] and baseline + equalizer [(b) 1500 r.p.m., (d) 3000 r.p.m., (f) 4500 r.p.m.] exhaust systems.

high-frequency flow noise at higher speeds and load, which could mask the effect of engine orders under certain conditions. Further studies are needed to quantify the flow noise in more detail.

Acknowledgements

The support provided for this work by Dr. F.H.K. Chen and D.W. Wendland of General Motors Corp. is gratefully acknowledged.

Appendix A. Dimensions of the exhaust system

Different sections of the baseline exhaust system are identified in Fig. 22, which also marks the location of equalizer on the right bank. Table 1 then provides the lengths and diameters (with the exception of catalytic converters and muffler for the latter) of these sections.

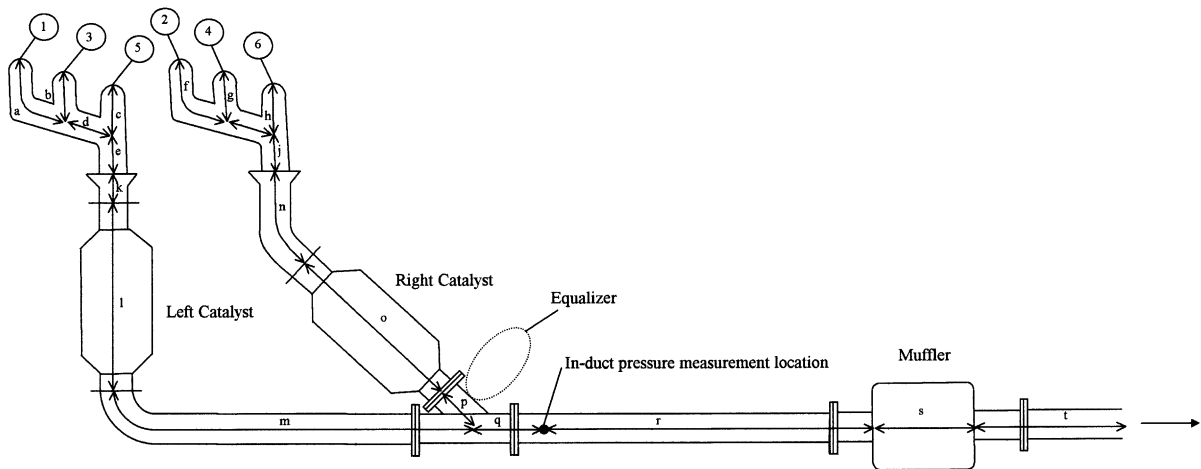


Fig. 22. GM 4.3L Vortec engine baseline exhaust system. The dimensions are given in Table 1.

Table 1
Length and diameters of exhaust system

Duct	Length (cm)	Diameter (cm)	Duct	Length (cm)	Diameter (cm)
a	20.32	3.8	k	30.48	5.7
b	7.62	3.8	l	29.21	Catalyst
c	10.16	3.8	m	93.98	5.96
d	17.78	3.8	n	38.1	5.7
e	5.08	3.8	o	29.21	Catalyst
f	33.02	3.8	p	32.39	5.96
g	7.62	3.8	q	10.16	6.1
h	10.16	3.8	r	120.6	6.1
i	10.16	3.8	s	63.5	Muffler
j	5.08	3.8	t	167.6	6.6

References

- [1] P. Hetherington, W. Hill, F. Pan, B. Sinder, E. Bradamante, G. Cerrato-Jay, Simulating odd fire V-10 exhaust noise for sound quality evaluation, SAE 1999-01-1652, 1999.
- [2] L.J. Ericksson, in: D.E. Baxa (Ed.), *Noise Control in Internal Combustion Engines*, Krieger, Florida, 1989 [Chapter 5].
- [3] B.S. Sridhara, M.J. Crocker, Review of theoretical and experimental aspects of acoustical modeling of exhaust systems, *Journal of the Acoustical Society of America* 95 (5) (1994) 2370–2393.

- [4] Y. Satyanarayana, M.L. Munjal, A hybrid approach for aeroacoustic analysis of the engine exhaust system, *Applied Acoustics* 60 (2000) 425–450.
- [5] F. Payri, A.J. Torregrosa, R. Payri, Evaluation through pressure and mass velocity distributions of the linear acoustical description of I.C. engine exhaust systems, *Applied Acoustics* 60 (2000) 489–504.
- [6] A. Selamet, V. Kothamasu, J.M. Novak, R.A. Kach, Experimental investigation of in-duct insertion loss of catalysts in internal combustion engines, *Applied Acoustics* 60 (2000) 451–487.
- [7] M. Hosomi, Analysis of pulsation inside pipe and study on exhaust sound characteristics of V type 8 cylinder engine, SAE 1999-01-1651, 1999.
- [8] L. Dedene, M.V. Overmeire, P. Guillaume, R. Valgaeren, Engineering metrics for disturbing sound elements of automotive exhaust noise, SAE 1999-01-1653, 1999.
- [9] A. Crewe, Tools for sound quality analysis in complex sound fields, SAE 941792, 1994.
- [10] E. Zwicker, H. Fastl, *Psychoacoustics: Facts and Models*, Springer, Berlin, 1990.
- [11] S.D.R. Corporation, *Sound Quality Version 3.1 Users Guide*, Structural Dynamics Research Corporation, Milford, Ohio, 1997.
- [12] E. Zwicker, H. Fastl, U. Widmann, K. Kurakata, S. Kuwano, S. Namba, Program for calculating loudness according to DIN 45631 (ISO 532B), *Journal of the Acoustical Society of Japan* 12 (1991) 39–42.
- [13] L.L. Beranek, Trans. Bull, Noise control in the office and factory spaces, in: *Proceedings of the 15th Annual Meeting of the Chemical Engineering Conference*, Vol. 18, 1950, pp. 26–33.
- [14] V.W. Aures, A procedure for calculating auditory roughness, *Acustica* 58 (1985) 268–281.
- [15] F.H. Kunz, Semi-empirical model for flow noise prediction on intake and exhaust systems, SAE 1999-01-1654, 1999.